Synergistic Silver Nanoparticle–Graphene Quantum Dot Composites in Silk Fibroin/Lathyrus Protein–Oxidized Alginate Hydrogels for Accelerated Diabetic Wound Healing

Parth Gulati,[1] Anuj Verma, [1] Safoora Zaffar,[2] Amiruddin Ali, [3] Sanjay Kumar Gupta,[4] Tatini Rakshit,[2] Shubha Banerjee,[3] and Suchetan Pal[1,5]*

**Corresponding author: suchetanp@iitbhilai.ac.in*

1. Department of Bioscience and Biomedical Engineering, Indian Institute of Technology-Bhilai, Durg, 491002, CG, India.

2. Department of Chemistry, Shiv Nadar Institution of Eminence, Greater Noida, 201314, UP, India.

3. Department of Plant Molecular Biology and Biotechnology, Indira Gandhi Krishi Vishwavidyalaya, Raipur 492012, Chhattisgarh, CG, India.

4. Department of Pharmacology, Rungta College of Pharmaceutical Sciences and Research, Bhilai 490024, Chhattisgarh, CG, India.

5. Department of Chemistry, Indian Institute of Technology-Bhilai, Durg, 491002, CG, India.

Supplementary figure section

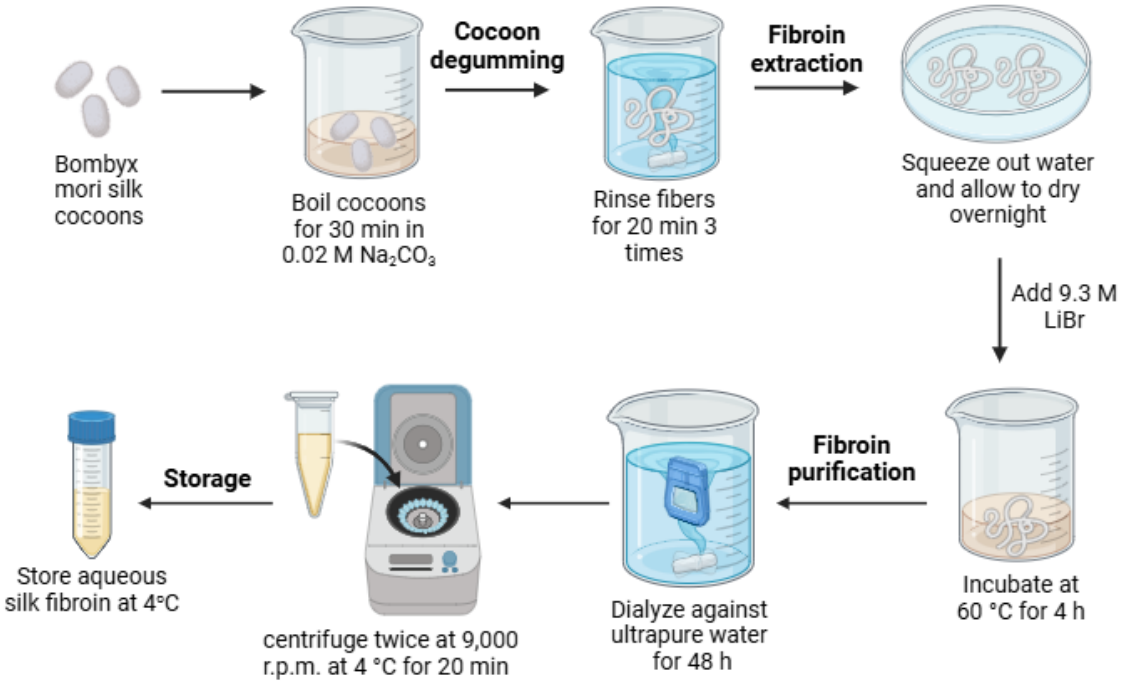

Fig. S1: Schematic illustration depicting the protocol for the extraction of Silk Fibroin protein

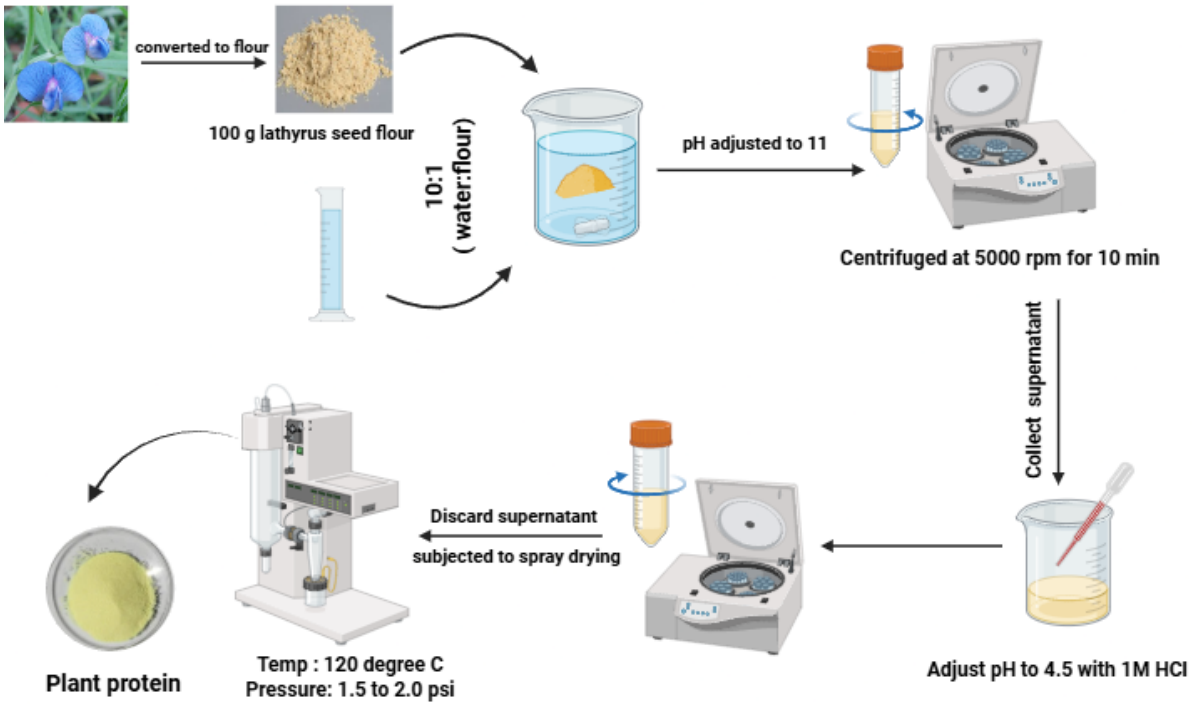

Fig. S2: Schematic illustration depicting the protocol for the extraction of Plant protein

Fig S3: Different combinations of antibacterial agent loaded (a) Plant-oAlg Hg, (b) Silk-oAlg Hg

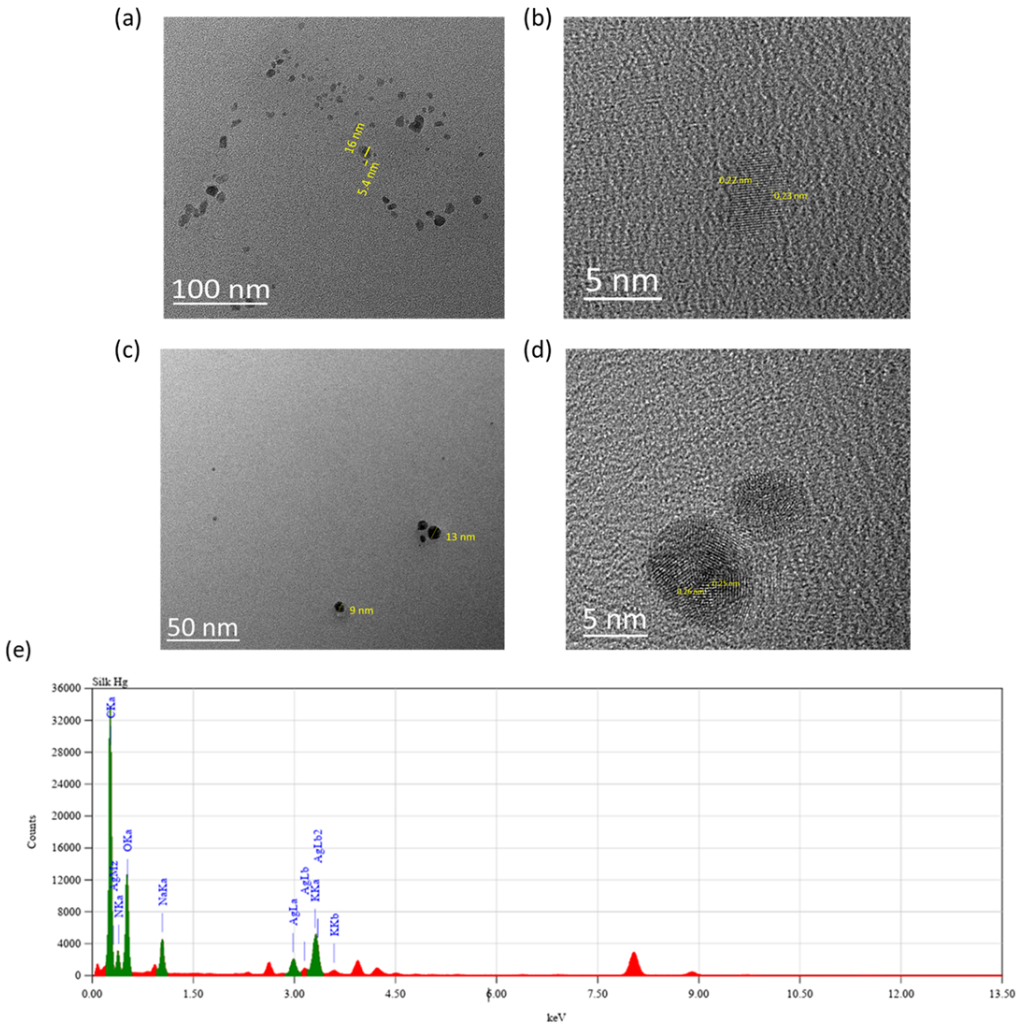

Fig. S4: a) TEM image of a) Graphene quantum dots (GQD) nps b) inter lattice distance of GQD nps. c) in-situ formed silver nanoparticles (Ag nps). d) inter lattice distance of Ag nps. e) EDX of formed silver nanoparticles.

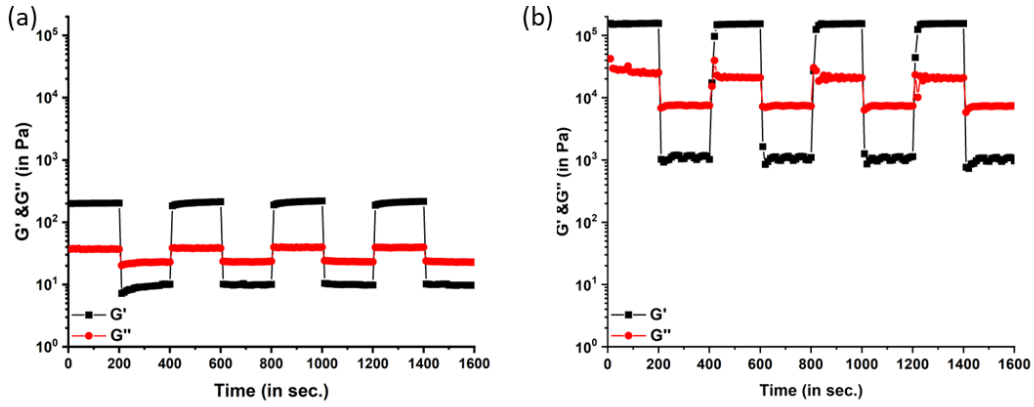

Fig. S5: (a-b) Shear stress recovery test for Silk-oAlg-HG and Plant-oAlg-HG) showing a shear thinning behaviour.

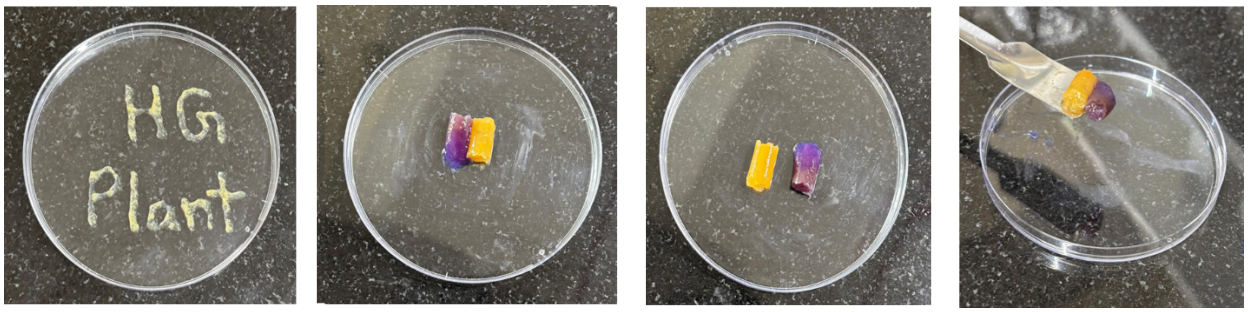

Fig. S6: Self-healing tendency of Plant-oAlg HG (healing time = 3 hrs)

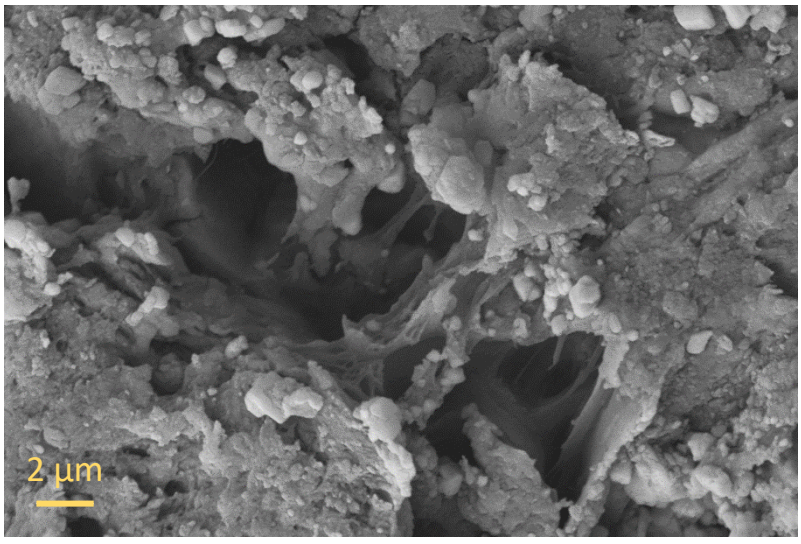

Fig. S7: FESEM images of plant protein-oAlg HGs

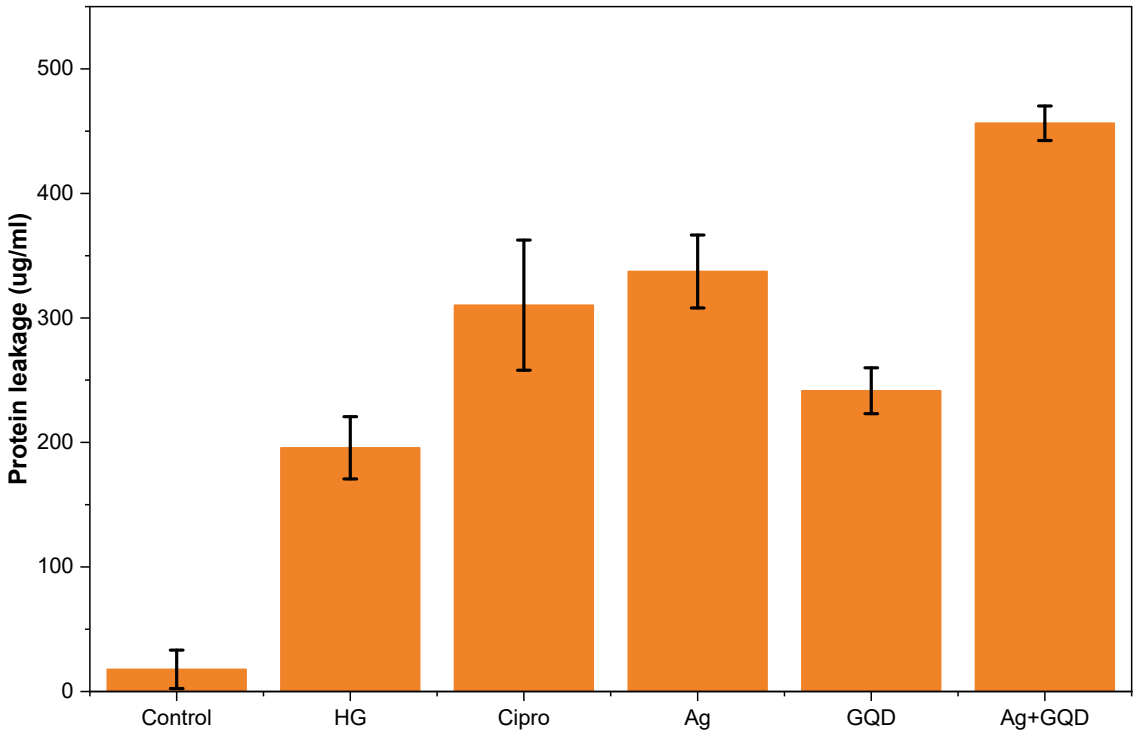

Fig S8. Protein leakage assay to determine the degree of bacterial membrane damage induced by different hydrogel formulations. The protein leakage was determined using the Bradford protein assay and was calculated as the protein concentration (µg/mL). The highest protein leakage was observed with the Ag+GQDs-loaded hydrogel, indicating the highest degree of bacterial membrane damage and antibacterial efficacy of the formulation compared to the individual treatments. Results are expressed as the mean ± SD (n = 3).

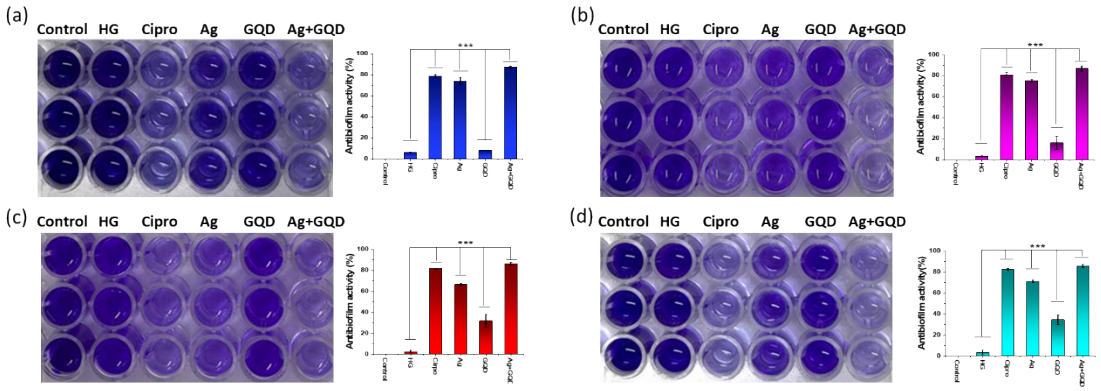

Fig. S9: Anti-biofilm assay performed in triplicate on various HG samples using crystal violet staining (a) Silk-oAlg HG with *E. coli*, (b) Plant-oAlg HG with *E. coli*, (c) Silk-oAlg HG with *M. luteus,* (d) Plant-oAlg HG with *M. luteus.*

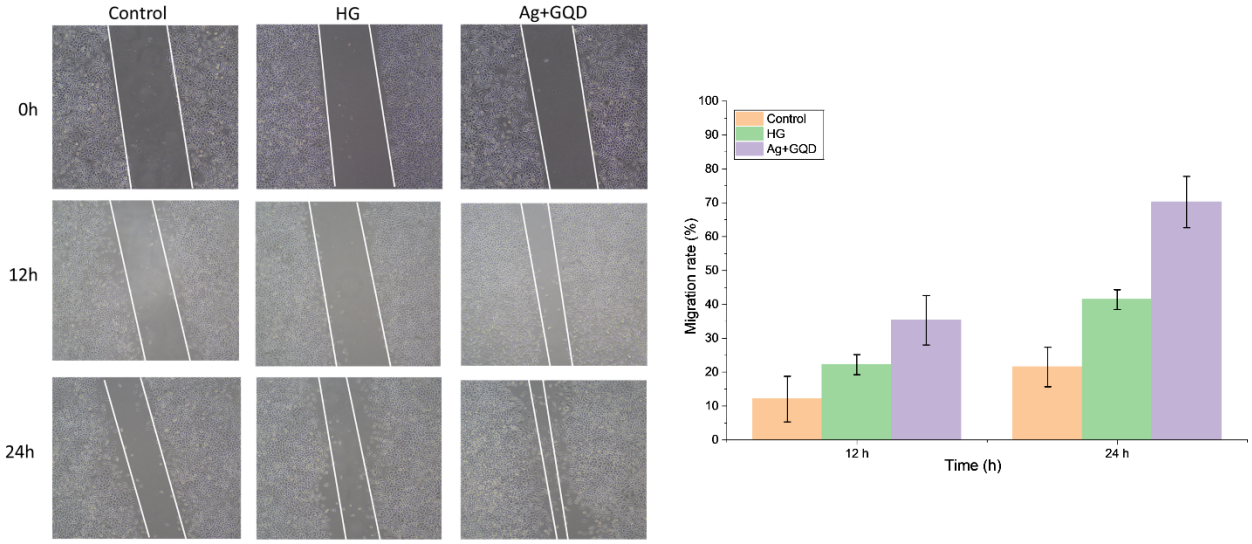

Fig. S10: Cell scratch assay demonstrating the fibroblast migration in presence of hydrogels.Representative optical microscopy images of L929 fibroblast monolayers showing wound closure in the control, hydrogel (HG), and Ag+GQD-incorporated hydrogel groups at 0, 12, and 24 h. Highest cell migration was observed in the Ag+GQD combination compared to HG and control group.

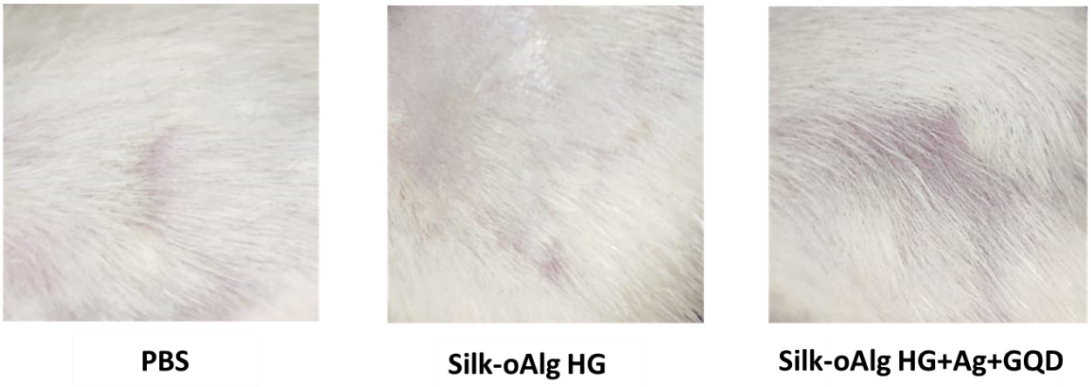

Fig. S11: Images showing no topical toxicity after applying Silk-oAlg HG on rat's skin

Supplementary table section

Antibacterial formulations	*E. coli*				*M. luteus*			
	Plant HG (colonies)	cfu/ml	Silk HG (colonies)	cfu/ml	Plant HG (colonies)	cfu/ml	Silk HG (colonies)	cfu/ml
HG	715	14.3×10^4	346	6.9×10^4	Lawn of bacteria	Too many to count	262	5.2×10^4
Cipro	5	1×10^3	5	1×10^3	6	1.2×10^3	10	2×10^3
Ag	10	2×10^3	24	4.8×10^3	7	1.4×10^3	14	2.8×10^3
GQD	19	3.8×10^3	38	7.6×10^3	205	4.1×10^4	19	3.8×10^3
Ag+GQD	1	2×10^2	3	6×10^2	1	2×10^2	1	2×10^2

Table S1: Quantification of antibacterial efficacy of plant and silk-based protein hydrogel against *E. coli* and *M. luteus* via CFU analysis.

Bacteria	Hydrogel System	Ag inhibition (%)	GQD inhibition (%)	Expected inhibition (Bliss) (%)	Observed Ag+GQD inhibition (%)	Interaction
E. coli	Plant HG	98.6	97.34	99.96	99.86	Additive
E. coli	Silk HG	93.04	88.99	99.2	99.13	Additive
M. luteus	Plant HG	97.31	21.15	97.9	99.62	Synergistic
M. luteus	Silk HG	94.62	92.69	99.7	99.62	Additive

Table S2. Bliss independence analysis of the interaction between silver nanoparticles (Ag) and graphene quantum dots (GQD) using data from the antibacterial plate assay. The Bliss independence model was used to predict the expected inhibition values for the interaction between Ag and GQD $E_{AB} = A + B - (A \times B)$, where A and B represent the inhibition fractions of the individual treatments. A comparison of the expected and observed inhibition values reveals an additive effect with some synergy against *M. luteus* in the plant hydrogel system.

Bacteria	Hydrogel	Ag (%)	GQD (%)	Bliss expected (%)	Observed Ag+GQD (%)	Interaction
E. coli	Plant HG	74.94	15.84	78.91	86.62	Synergy
E. coli	Silk HG	73.82	8.24	75.98	87.27	Strong synergy
M. luteus	Plant HG	71.25	34.57	81.19	85.69	Synergy
M. luteus	Silk HG	66.45	31.78	77.11	86.1	Strong synergy

Table S3. Bliss independence analysis of biofilm inhibition data evaluating the interaction between silver nanoparticles (Ag) and graphene quantum dots (GQD) in plant and silk hydrogel systems against *E. coli* and *M. luteus*. The expected inhibition was calculated using the Bliss independence model $E_{AB} = A + B - (A \times B)$, where A and B represent the inhibition fractions of Ag and GQD, respectively. Comparison of the predicted additive inhibition with the experimentally observed Ag+GQD inhibition demonstrates synergistic antibiofilm activity.